Heavy Nuclei in the Primary Cosmic Rays over Minnesota*

EIJI TAMAI
University of Minnesota, Minneapolis, Minnesota
(Received September 30, 1959)

An analysis of the heavy primary cosmic rays ($Z \geq 2$) has been made by using a stack of emulsions which was exposed at a high altitude on September 18, 1956, over Minnesota. In order to examine the low rigidity portion of the heavy primary cosmic rays, we have studied only the stopped particles in this stack. In this work, two methods to identify the charges of various particles have been employed: (1) track width measurement and (2) δ-ray density vs residual range. The energy spectra of α, L, and M groups in the primary cosmic radiation have been obtained. Their energy spectra show the existence of a maximum in each group, and the energy regions of the maxima increase with increasing charge of heavy element. Some possible interpretations of these spectra are discussed.

1. INTRODUCTION

IN order to obtain information about the origin of cosmic radiation and nuclear reactions in the stars, it is important to study the energy spectra and abundance of various components in the heavy primary cosmic radiation. However, while many experimental data concerning the heavy components of the primary cosmic radiation in the high rigidity region (Bev region) have been published, we have only little data on the low-energy portion excepting those on the α component studied by the Minnesota and Bristol groups[1–3] and those on the heavy components (α, M, and H nuclei) by the Tokyo and Chicago groups.[4] In particular, the latter group obtained the energy spectra of all of the heavy components, and found general resemblances of the shape including the existence of a maximum flux. The energy region of their maximum (500–600 Mev/nucleon) was somewhat different than that of the α component spectrum, that is, 250 Mev per nucleon, found by the former group.

In any event, it may give some insight into a mechanism of accelerating cosmic radiation, if we examine the existence of a maximum in the energy spectrum, the energy region of maximum, and the dependence of this energy region on the charge of the primary cosmic ray. The time variation should also be studied. In view of the above considerations, an investigation of the low rigidity heavy components of the primary cosmic radiation has been carried out at this laboratory. In this experiment, the emulsion stack was exposed at an altitude of 110 000 feet under a mean amount of matter of 6.7 g/cm² plus 0.3 g/cm² of packing material. This experiment deals with the energy spectra of α, L, and M groups and their relative abundance in primary cosmic radiation.

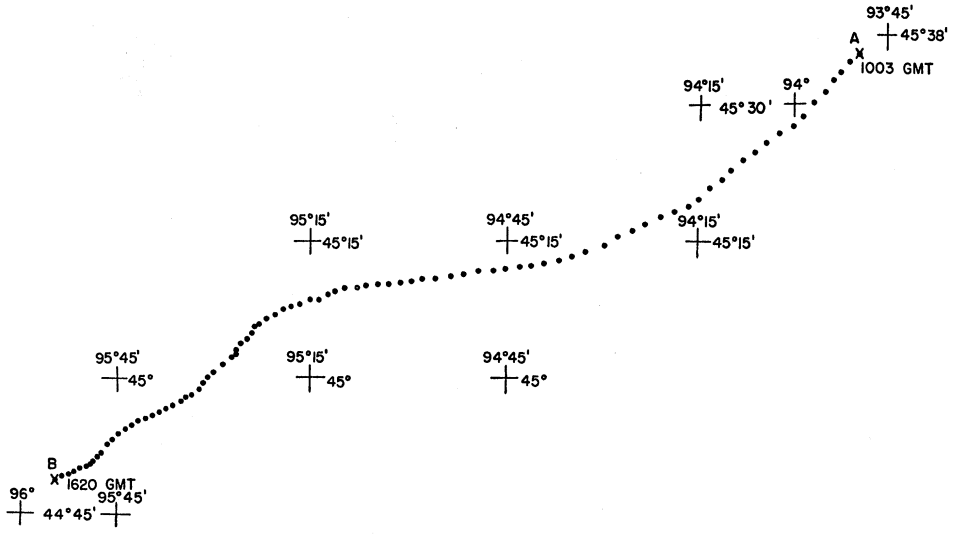

FIG. 1. Flight trajectory.

* This work was supported by the Office of Naval Research.
[1] Fowler, Waddington, Freier, Naugle, and Ney, Phil. Mag. **2**, 157 (1957).
[2] Freier, Ney, and Fowler, Nature **4619**, 1319 (1958).
[3] Fowler, Hillier, and Waddington, Phil. Mag. **2**, 293 (1957).
[4] Aizu, Fujimoto, Hasegawa, Koshiba, Mito, Nishimura, Yokoi, and Schein, Part I, (C, N, O group), Part II (H group), Part IV, α particles (to be published).

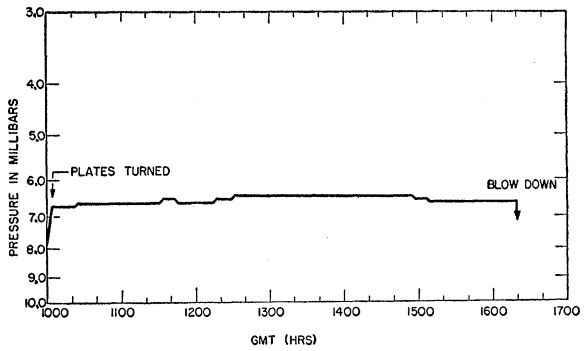

FIG. 2. Time-altitude curve for the exposure.

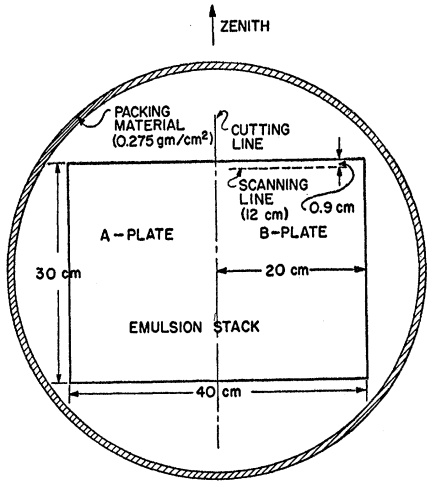

FIG. 3. The schematic drawing of the stack and the packing material.

2. EXPERIMENTAL PROCEDURE

1. Stack and Exposure Details

The stack of nuclear emulsions used to detect the particles in this work consisted of 300 stripped *G*5 emulsions with dimensions of 40 cm×30 cm×0.06 cm. It was exposed on September 18, 1956 over Minnesota; nominal geomagnetic latitude 55°N. The trajectory of the balloon is given in Fig. 1. The balloon reached ceiling altitude at 45.1°N and 93.8°W (geographic), and the stack was turned over and released at 44.8°N and 95.9°W. The flight curve is given in Fig. 2 where the pressure in millibars is plotted against the universal time, GMT. The pressure was measured by a Wallace Tierman gauge, photographed at 2 minute intervals, and by a code drum transducer supplied by Winzen Research, Inc. After recovery the emulsions were cut in two pieces (20 cm×30 cm×600μ) as shown in Fig. 3, and processed by the usual method of wet-hot stage at this laboratory. The minimum grain density observed in these plates was about 20 grains per 100μ.

2. Scanning

The emulsions were scanned along 12 cm and 0.9 cm from the top of the emulsion using 7×20 magnification. All particles crossing this line, satisfying the following geometric criteria, were recorded (Fig. 3).

1. The projected zenith angle in the emulsion plane does not exceed 30°.
2. The track length per plate in the zenith direction is equal to or larger than 3 mm.
3. δ-ray density is $\geq 0.7\delta$ rays per 100μ.

Every track recorded by the above criteria should have a minimum possible range of 10 cm or more in the stack before they come to the edge. The tracks were followed until they left the stack from the bottom side, stopped in the stack, or made interactions in it.

3. Determination of Charge

As is known, it is rather difficult to identify the charges and energies of the incident particles which make interactions or leave through the stack. For this reason, we have treated with only the particles which stopped in the emulsion.

The usual methods for determining the charge of a stopping track are as follows: 1. gap (or blob)-counting, 2. δ-ray density vs residual range, 3. the track width,

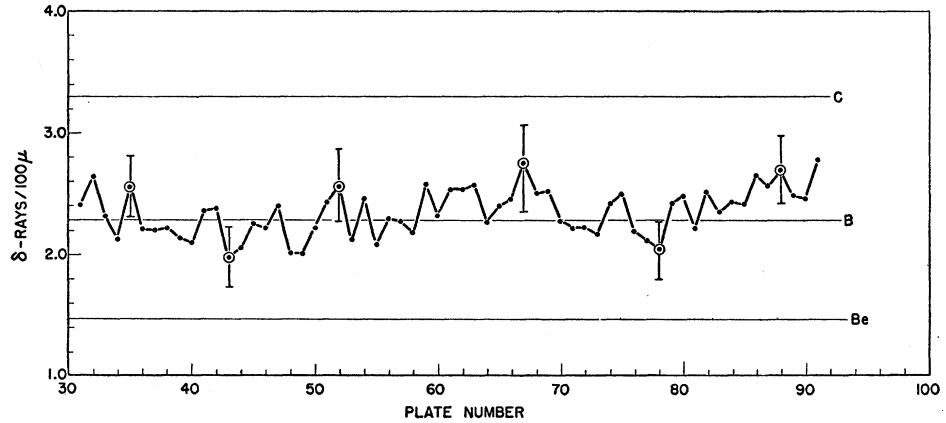

FIG. 4. δ-ray density measurement with the track which traverses 60 emulsions used in this experiment. The errors indicate the variability in individual emulsions.

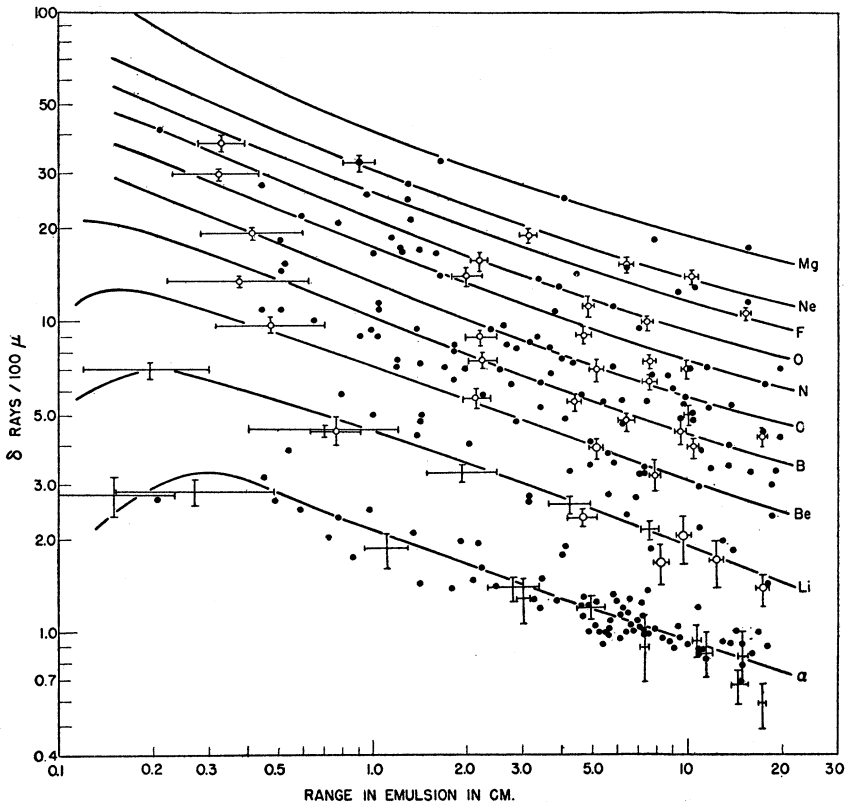

FIG. 5. The calibrations of the δ-ray density versus residual range. Plain crosses: data from the tracks of α's and Li^8. Open circles: data from the particles of which the charges were identified by their track width measurements.

4. the tapering length, and 5. variations of the above. In this experiment, both methods (2) and (3) have been employed independently.

a. δ-Ray Measurements

In order to establish the ionization calibration, however, the author starts with a track which is thought to be a relativistic boron from its observed interaction and its δ-ray density. In fact, this track penetrates through the 60 plates (27 cm) used in this work before it collides with a hydrogen atom or makes a peripheral collision with a heavier atom in the emulsion and breaks up into three relativistic particles, that is, two α particles and a proton. With this track, the δ-ray density in each plate was measured to examine the dependence of δ density on the development of the emulsion.

Figure 4 shows the results of the conventional 4-grain δ-ray counting on this track. The δ rays were counted over a length of 3 mm. The length was centered about the middle of the emulsion (in depth) and was more than 30μ away from either emulsion surface. From this figure, a correction for the variation of development can be made for the δ-ray density of each particle used. In the figure, the straight lines for the relativistic Be, B, and C, respectively, were obtained from Mott's formula:

$$n_\delta = 2\pi\left(\frac{e^2}{mc^2}\right)^2\left[\frac{mc^2}{W_1}-\frac{mc^2}{W_2}\right]\left(\frac{Z^2}{\beta^2}\right), \tag{1}$$

$$W_2 = 2mc^2\beta^2, \tag{2}$$

$$W_1 = 30 \text{ Kev}. \tag{3}$$

The calibration of charge determination by δ-ray density has been carried out in the following way. First of all, the δ-ray densities of the stopped particles which are easily recognizable as α particles are counted and plotted as a function of residual range. In addition, we have a favorable Be track which traverses about 4 cm in the stack before it collides with a proton and breaks up into a proton and a Li nucleus which makes a characteristic hammer track at the end point. The range of

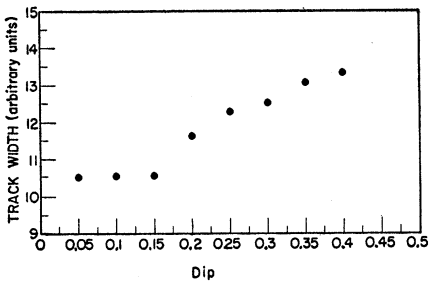

FIG. 6. Track width as a function of dip of the α-rays from radiothorium stars in the emulsions.

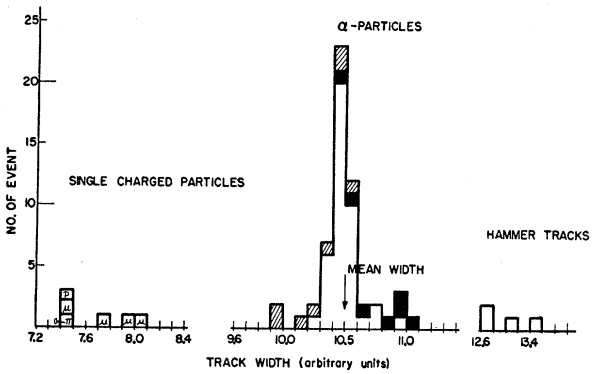

FIG. 7. Histogram of track width.

the Li^8 is 8.3 cm in the emulsion. Using this event, we can get a relation between δ-ray density and residual range for the Li track. Figure 5 gives the results for the α and Li particles. The theoretical curve for the δ-ray density versus residual range can be calculated by using the above formula (1), (2), and (3) and the range-energy relation.[5] The other data for Be, B, C, N, O, and Ne were obtained from the tracks which were identified as the corresponding particles, respectively, by the measurements of their track widths mentioned in the next paragraph. The black points in the figure show the data of all stopped particles which were recorded in this experiment. Every measurement of δ-ray counting was performed over a track length of at least 3 mm which was more than 30μ away from either emulsion surface.

b. Track Width Measurements

As for the calibration of track width, first of all, we measured the track widths of α particles emitted from Th nuclei in the emulsions by using the screw micrometer eyepiece.[6] In order to examine the variation of track width with increasing dip angle of track, the track widths of 127 α rays found in the several plates with different developments were measured. As one can see in Fig. 6, the track width stays constant, as long as the dip does not exceed 0.15 (after processing). Figure 7 represents the histograms of the track width of α rays, Li^8 particles and single charged particles, of which dips were ≤ 0.15. The shaded and the black areas show the α-ray tracks which were located within 20μ from the surface and the bottom of the emulsion, respectively. Although these areas may indicate a slight change in track width at the surface and the bottom of the emulsion, the deviation is so small ($\leq 5\%$) that they can be neglected for α-ray tracks located in the middle of the emulsion. We have examined the relation between charge and track width since 1954 and obtained the following experimental formula.[6]

$$W \propto \sqrt{Z}, \tag{4}$$

where W is the track width of a particle of charge Z. Recently, several investigators[7,8] have observed experimental results in good agreement with our formula, in analyzing the heavy fragments emitted from nuclear stars. The calibration of track width can be completed by determining the width of α rays. Figure 8 shows the distribution of track width for the heavy particles used in this work. From this figure, separation between par-

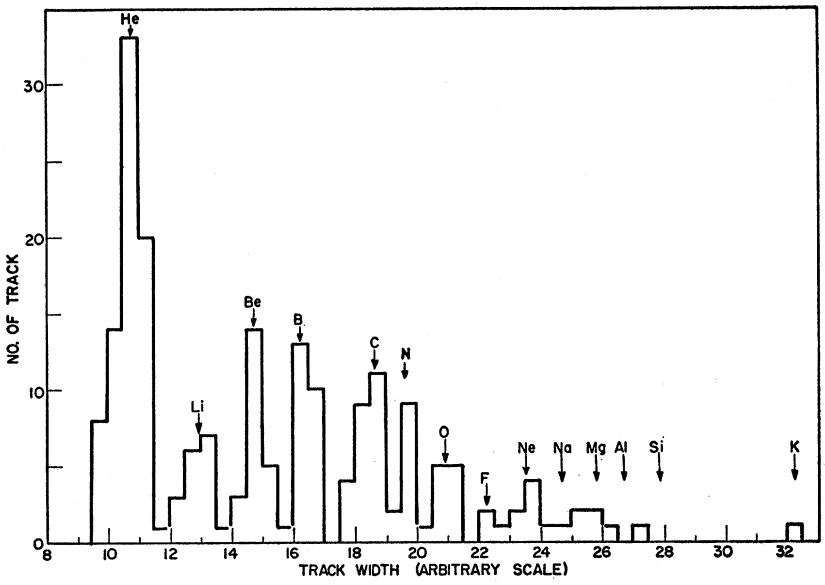

FIG. 8. Distribution of track width. The arrows show the widths estimated by Eq. (4).

[5] W. H. Barkas, University ofi California Radation Laboratory Report UCRL-ZN991-Rev (unpublished).
[6] Nakagawa, Tamai, Huzita, and Okudaira, J. Phys. Soc. (Japan) **11**, 191 (1956).
[7] O. Skjeggestad, Nuovo cimento **8**, 927 (1958).
[8] Barkow, Kane, O'Friel, and McDaniel (to be published).

ticles of neighboring charges can be obtained, though resolution between the particles in the heavy group is somewhat poor. The average widths of tracks for $Z=2$–14 were obtained and appear in Table I.

3. EXPERIMENTAL RESULTS

As the charges of the stopped particles were identified in the ways mentioned above, we can easily obtain the energies of them at the top edge of the stack by using the range-energy relation in the emulsion.[5] In Figs. 9 and 10 the energy spectra of the L (Li, Be, and B) and M (C, N, and O) groups in arbitrary frequency units are shown. In these figures, the energies were converted to those at the top of the atmosphere by taking into consideration the energy losses in air. In addition the number of particles found in the emulsions was corrected to the top of the atmosphere by multiplying by the factor;

$$\exp\left(\frac{R_{\text{emulsion}}}{\lambda_{\text{interaction}}}+\frac{(6.7+0.275)\sec\theta}{\lambda_{\text{absorption}}}\right). \quad (5)$$

The vertical air above the emulsion was 6.7 g/cm² and the packing material (glass fiber) was 0.275 g/cm². θ is the zenith angle. The values used for the interaction mean free paths in emulsion, $\lambda_{\text{interaction}}$ and the absorption lengths in air are shown in Table II.[2,9] Another correction is necessary. The energy interval for the particles which stop in the emulsion is different for different charges and when particles of several different charges are treated as a group a correction must be made at both ends of the observed energy range to account for the fact that some of the group members are observable while others are not. The corrections for this effect were made by using the observed relative abundances in the group in the energy range where all the group members are observable. As for the portion at the highest energy range, the spectrum has been obtained from the observed number of high-energy particles, in comparison with the integral energy spectrum[10];

$$N(>E)\propto(1+E)^{-1.4}. \quad (6)$$

Because of the poor statistics, especially in the H-group, a correction for the fragmentation processes in air has not been made. However, it is considered that it

TABLE I. The average widths of tracks for $Z=2$—14.

Z	Average width (μ)
2 He	0.66±0.015
3 Li	0.81±0.020
4 Be	0.93±0.017
5 B	1.04±0.017
6 C	1.16±0.017
7 N	1.23±0.018
8 O	1.33±0.017
9 F	1.41±
10 Ne	1.48±
11 Na	1.55±
12 Mg	1.61±
13 Al	1.67±
14 Si	1.73±

TABLE II. The interaction mean free paths in emulsion and the absorption lengths in air.

Interaction mean free path in emulsion (g/cm²)	Absorption mean free path in air (g/cm²)
$\lambda_\alpha=76.6$	$\lambda_\alpha=48.0$
$\lambda_L=59.4$	$\lambda_L=35.8$
$\lambda_M=50.9$	$\lambda_M=32.0$
$\lambda_H=36.4$	$\lambda_H=25.4$

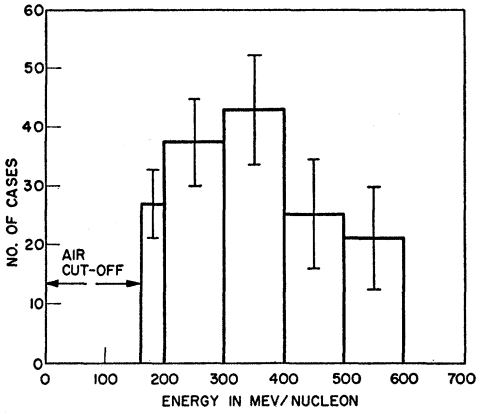

FIG. 9. The energy spectrum of the L-group (Li, Be, and B) at the top of the atmosphere.

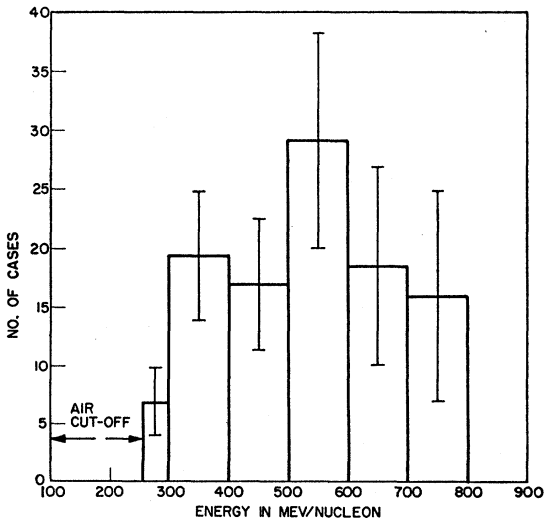

FIG. 10. The energy spectrum of the M-group (C, N, and O) at the top of the atmosphere.

[9] C. J. Waddington *et al.*, Phil. Mag. **3**, 19 (1958).

[10] Any disagreement between them has not been shown within the statistical error.

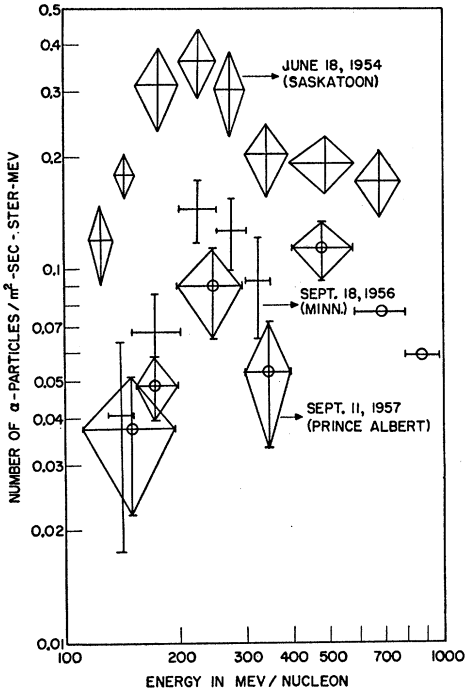

FIG. 11. The energy spectrum of the α particles at the top of the atmosphere.

can be neglected, since one intends to discuss only the shape of the energy spectrum.

Figure 11 shows the differential energy spectrum of α particles. The ordinate is given in units of particles/m^2 sec ster Mev and the abscissa is the energy per nucleon at the top of the atmosphere. In the figure, the data of other workers appear also.

From Figs. 9, 10, and 11, one can see that the energy spectra of all groups show a maximum in the differential flux. The position of the maximum tends toward higher energy with increasing charge from $\sim$230 to $\sim$550 Mev/nucleon, and also the energy spectra below the maxima fall off gradually, as the Minnesota group[1] and Koshiba *et al.*[4] observed. The relative abundance at the flight altitude (110 000 feet) is given for the observed particles with the charges of $Z \geq 3$ and the energies of $<$700 Mev/nucleon, and is shown in Fig. 12. It is remarked that the L group is the most abundant of all groups (L, M, and H groups) and the abundances of C and Ne nuclei dominate in M and H groups, respectively.

4. CONCLUSION AND DISCUSSIONS

The principal features of the data obtained in this work are:

(1) The energy spectra of α particles, L (Li, Be, and B) and M groups (C, N, and O) in the primary cosmic rays show peaks at energies around 200 to 300, 300 to 400 and 500 to 600 Mev/nucleon, respectively.

(2) These results do not indicate a sharp cutoff, but a gradual falloff of the spectrum at low energies.

(3) The dominant abundances of L group, C and Ne nuclei were observed. In discussing the results, we start with the energy spectra. The energy spectra of the primary particles obtained in the present experiment seem to be closely similar to other data,[1–4] as far as the existence of a maximum and the gradual decrease below the maximum are concerned. On the other hand, the peak positions of the spectra differ from each other. In fact, Koshiba *et al.*[4] found the maximum flux at $\sim$550 Mev/nucleon for the various components (α, M, and H groups) in disagreement with the data ($\sim$250 Mev/nucleon) for the primary α particles observed by the Minnesota and Bristol groups.[1] As a consequence, the former suggested that the maximum position might have been shifted to a higher energy by the effect of the magnetic storm. The comparison of our energy spectrum of α particles with that of the latter groups shows a similarity between the two, except for the flux values. (See Fig. 11.) In spite of this similarity, the maximum positions of L and M groups differ from that of the α group and are shifted to the higher energy side (Fig. 9 and 10).

Aside from this difference, the existence of a maximum and the gradual decrease below the maximum cannot be explained by geomagnetic or atmospheric effects, as has been discussed for the α particles, and it therefore seems likely that the energy spectra had the same shape before arriving in the vicinity of the earth.

However, in order to interpret the observed energy spectra, that is, the existence of the maximum position, we need another mechanism. First of all, we consider the screening mechanism. Namely, the existence of the maximum may be explained by the screening effect of the magnetic clouds emitted from the sun which prevent the particles with low magnetic rigidity from penetrating into the region of our observation. In this case, we should observe the maximum at the same magnetic rigidity for all kinds of charged particles. Furthermore, the position of the maximum should change according to the magnitude of the solar magnetic activity. These

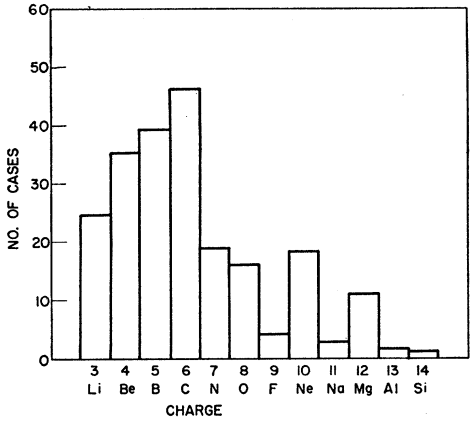

FIG. 12. The charge distribution of various particles observed at 110 000 feet.

deductions are incompatible with the results of the experiment, for the observed positions of the maxima of various particles differ from each other. Moreover, we can recall the results on the α particles which have been measured in 1954[1] and 1956. Even with the large differences of the solar activity between the two years, the maximum of the energy spectrum remained in the same position and the shape of the spectrum did not change appreciably although the intensity changed. Accordingly, it would be rather difficult to suppose that the observed spectrum had been made by the screening effect.

Although we cannot exclude definitely the screening mechanism, it is quite natural to consider the ionization loss in interstellar space as the second possibility. This process seems to be more plausible when we remember the energies of the maximum fluxes which were described in (1) of Sec. 4 and that of the H group obtained by Fowler *et al.*[3] Unfortunately the data are not sufficient to discuss this problem at length.

We now change the subject to the relative abundance of heavy primary cosmic rays. From Fig. 12 one can see the dominant abundance of the L group in comparison with the M and H groups. This would imply that the fragmentation process is favorable for the lower energy region which is measured in this experiment. In fact, this tendency has been observed in studies concerning the heavy fragments emitted from nuclear stars.[7,11] On the other hand, the dominant abundances of C and Ne nuclei in the M and H groups, respectively, were observed in the figure. As has been discussed for this point[4,12] the over abundance of them suggests that the ion-source of cosmic rays is probably due to a transient state in the evolution of stars.[13]

ACKNOWLEDGMENTS

The author would like to express his sincere thanks to Professor Edward P. Ney and Dr. Phyllis S. Freier for their constant interest and discussions. The author wishes to also thank Winzen Research, Inc., who made the balloon flight, and Mr. Sam Brinda, who developed the emulsions.

[11] Nakagawa, Tamai, and Nomoto, Nuovo cimento **11**, 780 (1958). E. Tamai, Nuovo cimento (to be published).
[12] Koshiba, Schultz, and Schein, Nuovo cimento **9**, 1 (1958).
[13] Burbidge, Burbidge, Fowler, and Hoyle, Revs. Modern Phys. **29**, 547 (1957).